Proceedings of the Second International Conference on Press-in Engineering 2021, Kochi, Japan – Matsumoto et al (eds)
 ISBN 978-1-032-10414-0

Experimental study on the pile group effect in the horizontal resistance of spiral piles

N. Ohnishi
Graduate School of Science and Engineering, Chuo University, Tokyo, Japan

H. Nishioka
Department of Civil and Environmental Engineering, Chuo University, Tokyo, Japan

ABSTRACT: Here, horizontal loading tests on spiral piles and cylindrical piles were conducted. The model ground was made using dry sand. Model piles were arranged in a row on the model ground; a wire was attached to the pile head and loaded monotonically in one direction. The experiment was conducted for five cases, with the center-to-center spacing of the piles changing from 1.5 times to 8 times the pile diameter. The results revealed that the tendency of the pile group effect of the spiral pile varied vastly depending on the evaluated load level. At the initial loading stage, spiral piles were more affected by the pile group effect than ordinary cylindrical piles; the relatively large initial displacement should be considered while designing spiral piles. However, as the loading progressed, spiral piles tended to have a smaller reduction in bearing capacity than the cylindrical piles owing to the pile group effect.

1 INTRODUCTION

1.1 *Background and objectives of the project*

Spiral piles are small-scale piles constructed by twisting flat steel plates that are used in the construction of pile foundations by manually drilling them into the earth's surface (Figure 1). It is very convenient in a site where the use of heavy construction machinery is arduous owing to a lack of space. An example of this could be a platform door foundation developed for railways using spiral piles (Nonaka et al. 2019), as shown in Figure 2.

When a pile group foundation is designed, it is necessary to consider the pile group effect fully. In practice, it is common to set the center-to-center interval of piles at a pile diameter (D) of approximately 2.5–3.0. However, most of the sites where spiral piles are used are narrow, and the area in which the foundation can be installed is limited. In the case of a pile group structure that uses spiral piles, a rational and economical design will be possible even if the pile spacing is smaller than the conventional pile spacing. However, only a few examples of horizontal loading tests on pile groups comprising spiral piles are available, and there are no studies in which the pile group effect was quantitatively investigated.

In the present study, horizontal loading tests on spiral and cylindrical piles were conducted, and the results were compared to examine the pile group effect of spiral piles.

2 EXPERIMENT OUTLINE

2.1 *Model pile*

A spiral pile made of phosphor bronze with a width of 20 mm, plate thickness of 2 mm, and length of 400 mm was utilized. The plate was twisted four times to make the pile (Figure 3). That is, the pitch is 50 mm. A separate (i.e., without sand) bending test demonstrated that the bending stiffness of this pile was EI = 2613.3 kN–mm^2. Figure 4 shows the bending test of a spiral pile. It can be confirmed that the localization of deformation has not occurred. Therefore, it assumes that the entire pile has uniform bending stiffness. In this experiment, all the spiral piles were grabbed by the fixing jig at pile head and fixed in the weak axis direction at the loading point, so the bending test was also fixed in the weak axis direction at the fixed part of the cantilever. A similar experiment was performed using an acrylic pile, which followed a conventional cylindrical pile model, with an

DOI: 10.1201/9781003215226-16

Figure 1. Construction status of spiral piles (Nonaka et al. 2019).

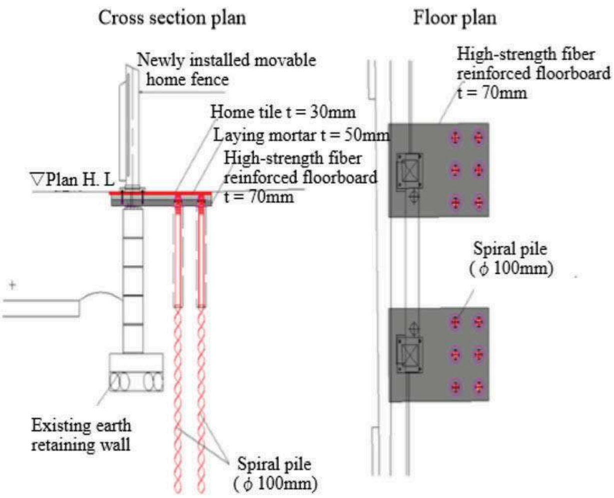

Figure 2. Example of foundation structure using spiral piles and high-strength fiber reinforced floorboards (Platform door foundation on embankment type platform) (Nonaka et al. 2019).

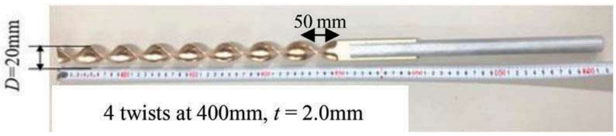

Figure 3. Model spiral pile.

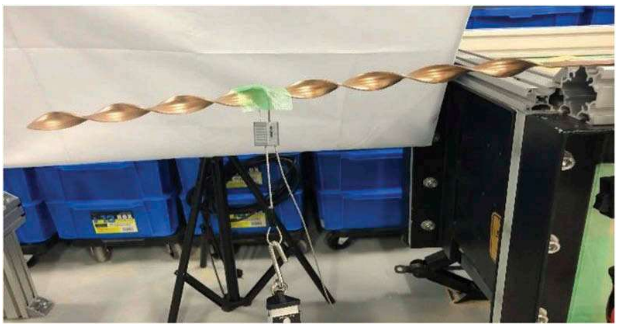

Figure 4. Bending test for spiral pile.

outer diameter of 20 mm and a plate thickness of 2 mm. The bending stiffness was found to be EI = 14838 kN–mm^2. The specifications of these models were set based on the following concepts. First, for the model acrylic pile, the pile diameter and plate thickness were set to satisfy $\beta l > 3$, a condition that can be generally treated as a semi-infinite length pile. β is the characteristic value of the pile represented by Equation (1). (Japanese Geotechnical Society. 2010)

$$\beta = [k_h \cdot D/(4EI)]^{1/4} \quad (1)$$

where k_h is the coefficient of the horizontal subgrade reaction, E is Young's modulus, and I is the moment of inertia of the area.

For k_h, the value obtained from a horizontal loading test result of a single pile conducted in advance was used. For the model spiral pile, the plate width was set to be the same as the outer diameter of the model acrylic pile. The plate thickness was set in proportion to the ratio of the plate width to the wall thickness of the actual spiral pile.

2.2 *Experimental device*

The model ground was made using dry sand. The sand was dropped into a soil tank with a width of 1000 mm and a depth of 400 mm using the multiple sieving method. The relative density of the sand was approximately 80%.

In the model pile installation method, the spiral piles were individually drilled into the model ground to a total penetration depth of l = 390 mm. The acrylic pile penetrated 150 mm when 200 mm of sand was poured; then, the remaining sand was poured. (Therefore, the penetration depth, l, was 350 mm).

The spiral pile was constructed using the jig shown in Figure 5, but due to the influence of the problem in the design, blurring and over-rotation inevitably occurred during construction.

Model piles were arranged in a row on the model ground, and a wire was attached to the pile head and loaded monotonically in one direction (Figure 6,7). The experimental condition is that the pile head and tip are free.

2.3 *Experimental pattern*

The experiment was conducted for five cases, with the center-to-center spacing of the piles changing from 1.5 times to 8 times the pile diameter D (Figure 8). For spiral piles, D was set to the width of the plate.

As shown in the figure, all spiral piles were constructed to be in the weak axis direction at the loading point.

To improve the reliability of the results, acrylic piles and spiral piles were tested three times in all cases.

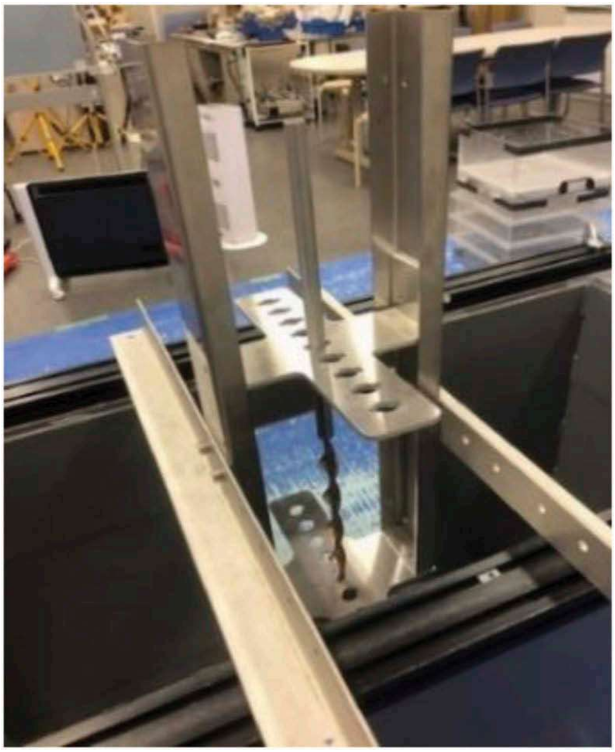

Figure 5. Construction jig for spiral pile.

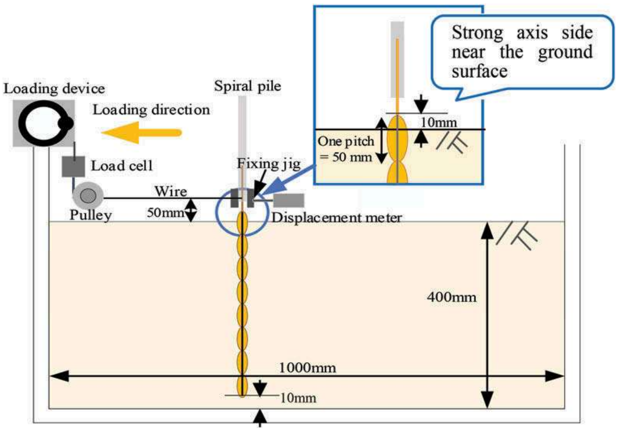

Figure 6. Overview of the test soil tank and loading device.

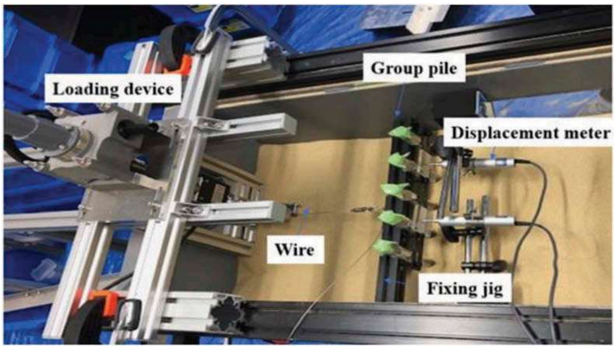

Figure 7. Installation status of loading equipment and measuring equipment.

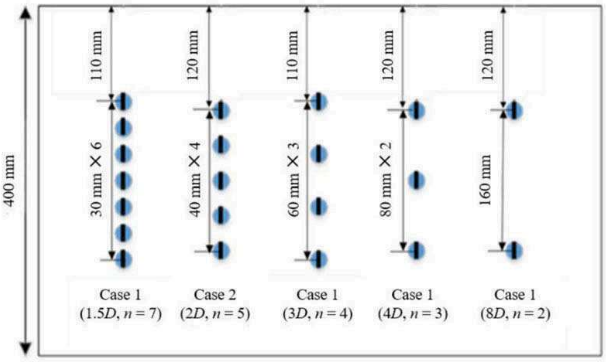

Figure 8. Experimental case pile placement.

3 EXPERIMENTAL RESULT

3.1 *Acrylic pile*

Figure 9 shows the load–displacement relationship of the acrylic piles. Although it differs slightly from test to test, the resistance decreases as the pile spacing reduces, owing to the pile group effect.

3.2 *Spiral pile*

Conversely, from the load–displacement relationship curves of the spiral piles shown in Figure 10, in some cases, the resistance per pile obtained from the experiment conducted at $L = 1.5D$ exceeded the resistance obtained at $L = 8D$; the resistance did not decrease even if the pile spacing was reduced. We will discuss these differences in chapter 4.

3.3 *Pile characteristic value βl*

For the test results of $L = 8D$ of the acrylic pile, the value of βl was calculated from the average value of the load when the horizontal displacement was 0.2 mm. The Chang formula (Japanese Geotechnical Society. 2010) used is shown in Equation (2).

$$y_t = \frac{(1+\beta \mathrm{h})^3 + 1/2}{3EI\beta^3} P \tag{2}$$

where y_t is the horizontal displacement, β is the characteristic value of the pile, h is the height of the loading point, E is Young's modulus, I is the moment of inertia of the area, and P is the load.
From the equation, $\beta l = 3.89$ ($l = 350$ mm) was obtained. It was found that the setting concept of the model specification ($\beta l > 3$) was satisfied when the coefficient of the horizontal subgrade reaction at this time was calculated for $k_h = 55609$ kN/m^3.
Similarly, βl and k_h for the spiral pile were obtained to be $\beta l = 7.72$ ($l = 400$ mm) and $k_h = 72510$ kN/m^3. It was observed that the flexural rigidity was lower than that of acrylic piles and βl was larger owing to the longer l, but k_h itself was higher

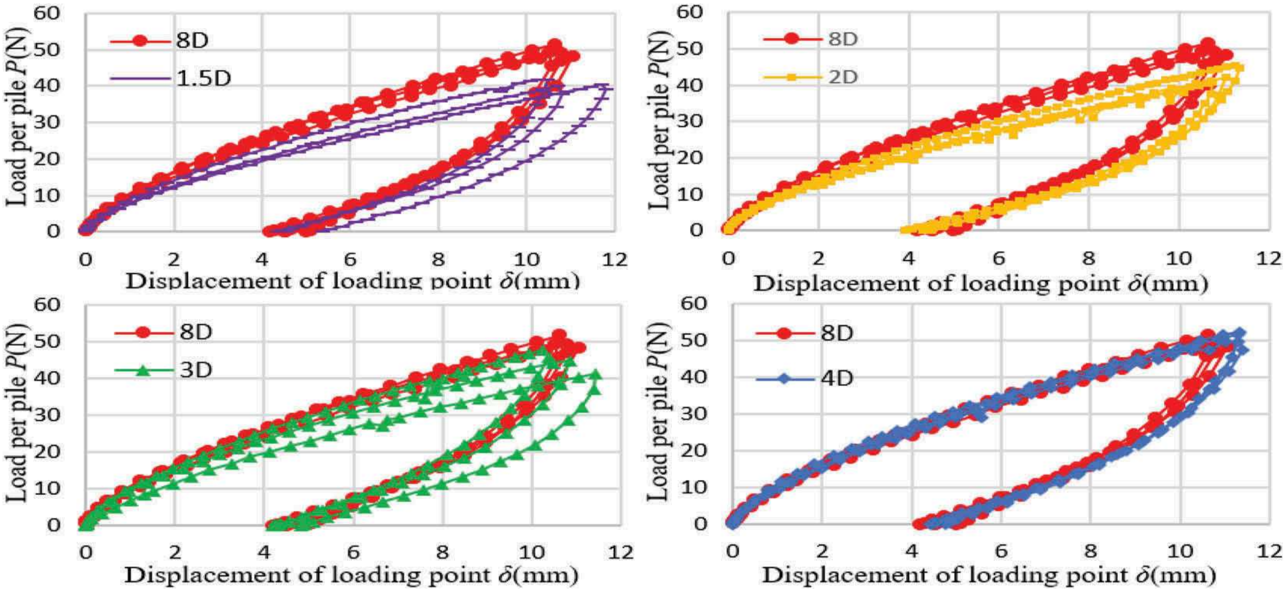

Figure 9. Acrylic pile load–displacement relationship.

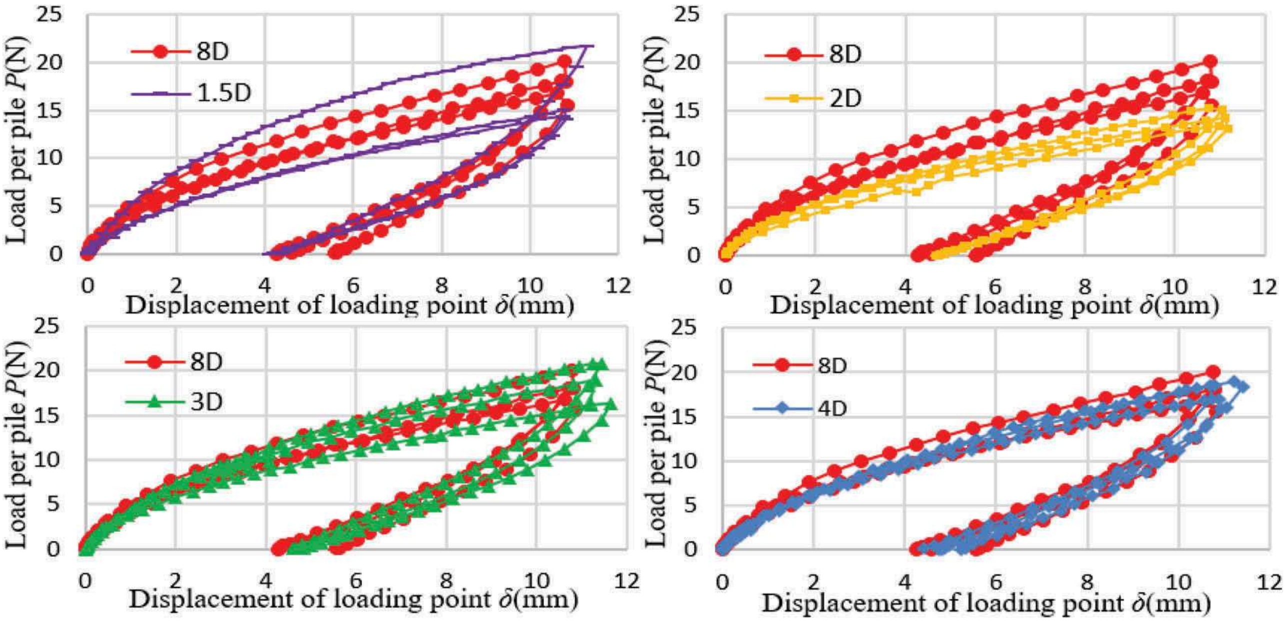

Figure 10. Spiral pile load–displacement relationship.

than that of acrylic piles owing to the influence of load-width dependence. (Japanese Geotechnical. 2017)

4 DISCUSSION OF EXPERIMENTAL RESULTS

4.1 *Large load*

The behavior when the ground resistance was sufficiently plasticized was compared (hereinafter referred to as “large load”). Table 1 shows the experimental results and coefficient of variation of the acrylic pile under a 40 N load. Table 2 shows the experimental results and coefficient of variation of the spiral pile when 14 N is loaded.

Table 1 shows that the experimental results of the acrylic piles are relatively stable, although there is some variation at the pile center spacing $L = 3D$.

Conversely, Table 2 shows that the results of spir al piles are more inconsistent than those of acrylic piles. The possible causes could be the construction failure of the pile and disturbance of the ground around the pile during rotational penetration. Notably, for spiral piles, slight differences in construction conditions, such as the amount of force applied during rotational penetration and the slight deviation of the pile center, may significantly affect the

Table 1. Displacement of the acrylic pile under 40 N load.

Pile center spacing	P = Displacement when 40 N is loaded (mm)			Average	Coefficient of variation
$L = 8D$	7.79	8.17	7.36	7.77	4%
$L = 4D$	7.96	7.69	7.42	7.69	3%
$L = 3D$	9.00	8.01	10.96	9.32	13%
$L = 2D$	10.42	10.18	9.27	9.96	5%
$L = 1.5D$	9.66	10.70	11.49	10.61	7%

Table 2. Displacement of the spiral pile under 14 N load.

Pile center spacing	P = Displacement when 14 N is loaded (mm)			Average	Coefficient of variation
$L = 8D$	8.37	5.96	7.39	7.24	14%
$L = 4D$	6.47	7.72	7.00	7.06	7%
$L = 3D$	5.77	5.69	8.95	6.80	19%
$L = 2D$	9.45	10.74	11.42	10.54	8%
$L = 1.5D$	4.45	9.62	10.10	8.06	32%

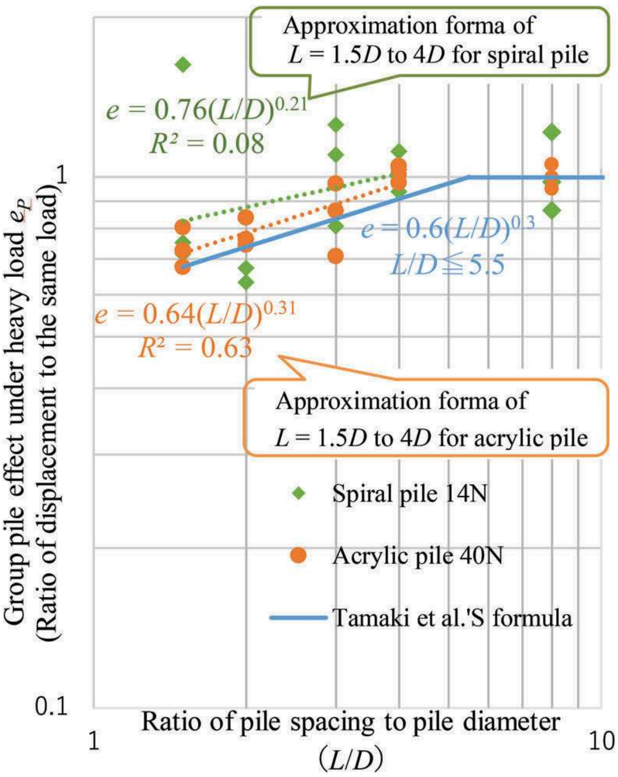

Figure 11. Relationship between pile spacing and group pile effect e_p under large load.

development of resistance. Therefore, there is a possibility that the disorder of construction when using the construction jig described in Chapter 2 had a significant influence. Remarkably, at $L = 1.5D$, which has the closest pile spacing, the results varied widely; the peripheral ground of the pile was strongly compacted during the rotational penetration, and the resistance increased.

However, it is difficult to eliminate this blurring and over-rotation even in the actual field. Therefore, although it is necessary to consider the uncertainty associated with construction in the design, it is important for research to separate construction variation from other factors.

Figure 11 shows the relationship between pile spacing and pile diameter, the L/D ratio, obtained in this experiment, and the pile group effect, e_P, under a large load. The pile group effect e_P on the vertical axis in Figure 11 is the value obtained by dividing the displacement of a single pile under the same load by the displacement of the pile group, referring to the definition by Tamaki et al (1971). However, in this experiment, the average of the cases with the pile center-to-center spacing $L = 8D$ was set to be the same as that of a single pile without the pile group effect. Figure 9 shows the pile group effect when 14 N is loaded on the spiral pile and 40 N is loaded on the acrylic pile. Further, Figure 11 also illustrates the relational expression between the pile spacing and the pile group effect in the case of the free pile head given by Tamaki et al (1971). shown in Equation (3).

$$e = 0.6(L/D)^{0.3} \quad 5.5 > (L/D) > 1.5 \tag{3}$$

where e is the pile group effect, L is the pile center spacing, and D is the pile diameter. In addition, in Figure 9, the results of approximating the $L = 1.5D$ to $4D$ data in both cases with a power function are shown according to Equation. (3).

From Figure 11, we understand that the result of the acrylic pile is relatively close to the relational expression of Tamaki et al (1971). Conversely, the spiral pile has a larger average e_P value of the pile group effect than the acrylic pile. Furthermore, because the spiral pile has a smaller index value in the approximation formula than the acrylic pile, it was found that the effect of the pile interval on the pile group effect was relatively small when evaluated under a large load. However, the value of the coefficient of determination, R^2, is very low owing to the large variation in the results.

The reason for this difference could be that the stress distribution range in the ground near the spiral pile is smaller than that of the conventional cylindrical pile. It is predicted that this is because there are points where the effective width of the spiral pile when pushed into the ground is reduced to the plate thickness instead of the full width. Moreover, since the projected area of the loading direction of the $1/\beta$ section of the spiral pile is smaller than the cylindrical pile, D can be evaluated to be smaller than the plate width, and as a result, there is a possibility that a difference in the group pile effect appears.

4.2 *Initial stage of loading*

Next, to consider the difference in tendency when the load level to be evaluated is reduced, the pile group effect at a displacement of 1% (0.2 mm) of the pile diameter is evaluated (Figure 12,13). This displacement level is generally treated as an equivalent linear range in design practice. Therefore, we focus on the horizontal spring constant K obtained by dividing the horizontal load by the horizontal displacement.

Table 3 shows the horizontal spring constant of the acrylic pile, and Table 4 shows the horizontal spring constant of the spiral pile when displaced by 0.2 mm. There is no significant difference in the variation in the results of the acrylic pile and the spiral pile, unlike in the case of a large load.

Figure 14 shows the relationship between pile spacing L/D and horizontal spring constant pile group effect e_K when the pile diameter is displaced by 1% (0.2 mm). Pile group effect e_K on the vertical axis is the ratio of the horizontal spring constant at 0.2 mm displacement of $L = 8D$ to the average of all three cases with the other horizontal spring constants, where the L values are $4D$, $3D$, $2D$, and $1.5D$.

Figure 14 shows that the acrylic pile has a greater pile group effect than the spiral pile. In particular, for acrylic piles, the effect was very large at the initial stage of loading.

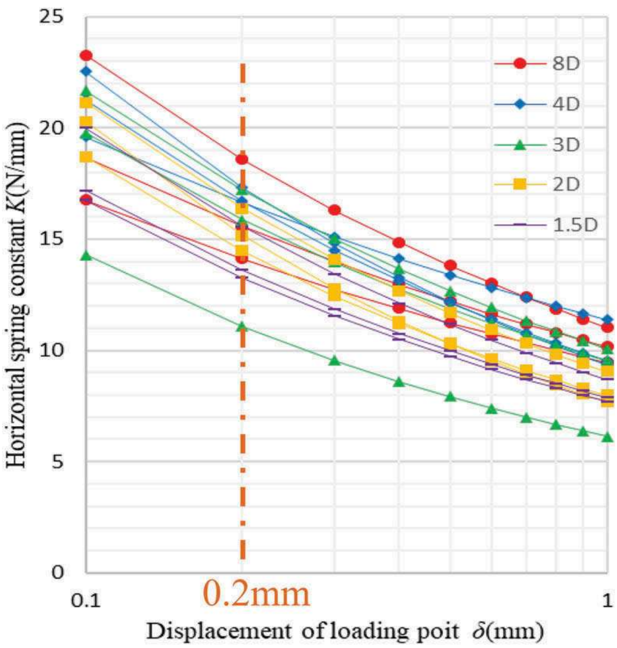

Figure 12. Relationship between displacement and horizontal spring constant of acrylic pile.

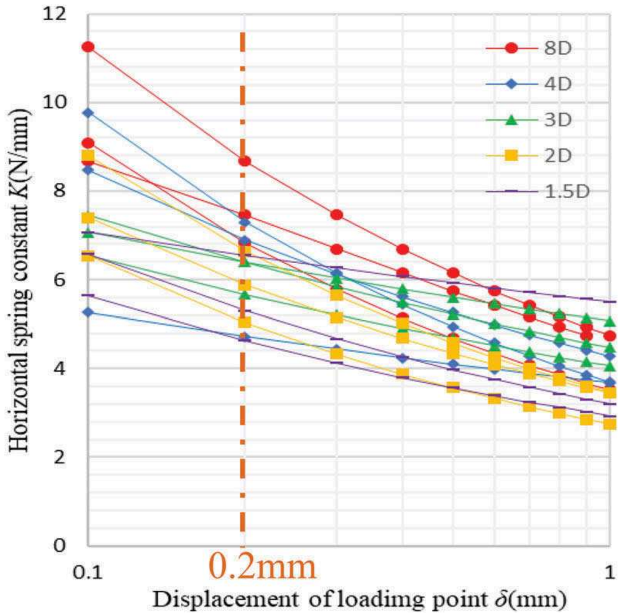

Figure 13. Relationship between displacement and horizontal spring constant of spiral pile.

Table 3. Horizontal spring constant at 0.2 mm displacement of acrylic pile.

Pile center spacing	Horizontal spring constant at 0.2 mm displacement K (N/mm)			Average	Coefficient of variation
$L = 8D$	15.56	14.11	18.58	16.08	12%
$L = 4D$	17.30	16.70	16.63	16.88	2%
$L = 3D$	15.88	17.21	11.09	14.73	18%
$L = 2D$	15.15	14.47	16.37	15.33	5%
$L = 1.5D$	15.57	13.60	13.26	14.14	7%

Table 4. Horizontal spring constant at 0.2 mm displacement of spiral pile.

Pile center spacing	Horizontal spring constant at 0.2 mm displacement K (N/mm)			Average	Coefficient of variation
$L = 8D$	8.68	6.58	6.83	7.36	13%
$L = 4D$	4.72	7.29	6.90	6.30	18%
$L = 3D$	6.39	6.39	5.67	6.15	6%
$L = 2D$	5.88	6.64	5.04	5.85	11%
$L = 1.5D$	6.55	4.63	5.30	5.49	14%

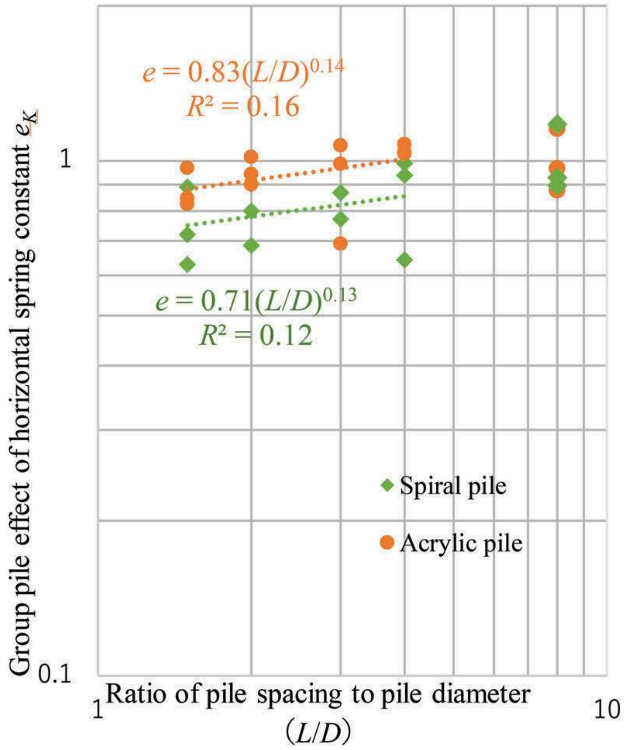

Figure 14. Relationship between pile spacing and horizontal spring constant group pile effect e_K.

Figure 15. New construction jig for spiral pile.

5 CONCLUSIONS

Examination of the pile group effect of spiral piles revealed that the effect varied significantly depending on the evaluated load level. Designs must consider that at the initial stage of loading, spiral piles are more affected by the pile group effect than ordinary cylindrical piles, and the initial displacement is relatively large. However, as the loading progressed, it was found that spiral piles tended to have a larger pile group effect than the cylindrical acrylic piles.

The test results for spiral piles vary widely, and slight differences in conditions at the time of penetration may significantly affect the resistance. Therefore, great care should be taken when constructing spiral piles.

In our future studies, we will use the new construction jig shown in Figure 15 and conduct experiments to reduce construction disturbances. In addition, we will conduct experiments that simulate actual construction conditions, such as horizontal load tests with multiple rows of pile groups that match the bending rigidity of spiral piles and acrylic piles, to explain the pile group effect of spiral piles further.

REFERENCES

Japanese Geotechnical Society: *Method for Lateral Load Test of Piles*, pp32 Maruzen Publishing, 2010. (in Japanese)

Japanese Geotechnical Society: *Soil and Foundation Design Calculation Exercises Corresponding to New Design Methods (2017 edition)*, pp75 Maruzen Publishing, 2017. (in Japanese)

Nonaka, T., Tsushima, F., Maehara, S., Nishioka, H., Otsuka, K., Inoyae, Y., Sugawara, T., Fujita, M. 2019. Proposal of home door foundation structure using spiral pile and high strength fiber reinforced slab. *JSCE the 74th Annual Lecture, VI-851*. (in Japanese)

Tamaki, S., Mitsuhashi, K., Imai, T. 1971. Horizontal resistance of a pile group subjected to lateral load. *Proceedings of JSCE 192:* 79–89. (in Japanese)